J. Membrane Biol. 190, 133–144 (2002)
DOI: 10.1007/s00232-002-1033-5

The Journal of
Membrane
Biology

Somatic Gene Transfer of Tagged K^+ Channel Fragments to Probe Trafficking and Electrical Function in Epithelial Cells and Cardiac Myocytes

N. Neyroud[1], I. Deschênes[1], M. Akao[1], H.B. Nuss[2], E. Marbán[1]
[1]Institute of Molecular Cardiology, The Johns Hopkins University School of Medicine, 844 Ross Bldg., 720 N Rutland Ave., Baltimore, MD 21205, USA
[2]Cardiology Research Group, University of Maryland School of Medicine, Baltimore, MD 21201, USA

Received: 1 April 2002/Revised: 31 July 2002

Abstract. To evaluate the roles of the C-termini of K^+ channels in subcellular targeting and protein-protein interactions, we created fusion constructs of the cell-surface antigen CD8 and the C-termini of Kv4.3, Kv1.4 and KvLQT1. Using a Cre-*lox* recombination system, we made 3 adenoviruses containing a fusion of the N-terminal-and transmembrane segments of CD8 with the C-termini of each of the 3 K^+ channels. Expression in polarized Opossum Kidney (OK) epithelial cells led to localization of CD8-Kv4.3 and CD8-Kv1.4 into the apical and basolateral membranes, while CD8-KvLQT1 remained in the endoplasmic reticulum (ER), even when co-expressed with MinK. When expressed in rat cardiac myocytes in culture, all the 3 constructs were diffusely targeted to the surface membrane. The ER retention of CD8-KvLQT1 in OK cells but not in cardiomyocytes thus reveals functional differences in trafficking between these two cell types. To probe functional roles of C-termini, we studied K^+ currents in cardiac myocytes expressing CD8-Kv4.3. Patch-clamp recordings of transient outward current revealed a hyperpolarizing shift of steady-state inactivation, implying that CD8-Kv4.3 may be disrupting the interaction of Kv4.x channels with one or more as-yet-undefined regulatory subunits. Thus, expression of tagged ion-channel fragments represents a novel, generalizable approach that may help to elucidate assembly, localization and function of these important signaling proteins.

Key words: K^+ current — Cell targeting — Epithelial cells — Cardiac myocytes — C-terminus — Gene transfer

Correspondence to: E. Marbán; email: marban@jhmi.edu

Introduction

Potassium channels constitute the largest and most diverse group of ion channels (Rudy, 1988; Hille, 1992). They are composed of variable combinations of subunits and their subunits associate with numerous regulatory proteins. Because of this diversity, K^+ channels play a major role in determining the specific phenotypes of excitability in neurons, cardiac myocytes and other electrically-active cells. Part of this complexity is conferred by distinct roles of various structural domains of K^+ channel alpha-subunits in cell targeting and subunit assembly. The N-terminal regions of various K^+ channels are known to take part in homo- and heteromultimerization (Strang et al., 2001), but the role of the C-termini is less clear. Nevertheless, it has been shown that some ion channel C-termini are responsible for the targeting of the proteins to their subcellular localization by interacting with auxiliary proteins (Zito et al., 1997; Li, Takimoto & Levitan, 2000).

To evaluate the roles of C-termini of voltage-dependent K^+ (Kv) channels in protein-protein interactions, including those that determine subcellular addressing of channels, we created fusion constructs of the cell surface antigen CD8 and the C-termini of Kv4.3, Kv1.4, and KvLQT1, three cardiac K^+ channels that play an important role in cardiac repolarization. The idea is to link a robust extracellular epitope and a transmembrane domain to a defined intracellular domain; epifluorescence microscopy can then track the fate of the intracellular C-termini, either in living intact cells for surface expression or in permeabilized cells. Our first goal was to assess subcellular localization of the various constructs in a polarized cell type, for which we chose Opossum Kidney (OK) cells. OK cells form polarized monolayers with epithelial properties in culture and are a

classical model system to study the targeting of heterologous membrane proteins of both epithelial and neuronal origin (Reshkin et al., 1990). Indeed, they reproduce neuronal subcellular localization, with the apical membrane being like the axonal one and the basolateral membrane being like the dendritic one (Dotti & Simons, 1990). We chose to study Kv1.4 and Kv4.3 channels in epithelial cells because Kv1.4 and Kv4.2 (which is very close to Kv4.3 but is neuronal) are known to have specific localizations in neurons: Kv1.4 is addressed to axons and Kv4.2 to dendrites (Sheng et al., 1992). Next, to assay the functional consequences on ionic currents, we expressed the CD8-Kv4.3 fusion construct in rat heart cells. Such cells have robust transient outward current (I_{to}) encoded by members of the Kv4 family (Apkon & Nerbonne, 1991; Faivre et al., 1999), so that any functional effects of C-terminal overexpression should be evident. The Kv4 family was of particular interest, as it encodes an I_{to} that is dynamically regulated during development (Wickenden et al., 1997) and in pathologic states of hypertrophy and heart failure (Wickenden et al., 1998).

Our results indicate that K^+ channel C-termini can influence subcellular localization in a manner that varies with cell type. More interestingly, we find that I_{to} gating properties are altered by C-terminal overexpression. Thus, this gene transfer approach constitutes a new, generalizable tool to probe the trafficking and function of defined protein regions.

Materials and Methods

Plasmid Construction and Adenovirus Preparation

The adenovirus shuttle vectors pAdEcd, pAdVgRXR, pAdEcdKv4.3 and pAdCGI-MinK (Hoppe, Marban & Johns, 2000; 2001) have been described elsewhere. Briefly, the pAdEcd plasmid contains an ecdysone-inducible promoter and the pAdVgRXR plasmid provides the ecdysone and the retinoid X receptors that bind to the ecdysone promoter and induce transcription. The pAdCGI-MinK provides both the genes encoding the green fluorescent protein (GFP) and MinK, the GFP gene being cloned behind an internal ribosome entry site (IRES) (Pelletier & Sonenberg, 1988; Jang et al., 1989).

The N-terminal and transmembrane domains of the human CD8 coding sequence (amino acids 1 to 222) were cloned into the multiple cloning site of pAdEcd to generate pAdEcd-CD8trunc. The C-terminal regions of the rat Kv4.3 cDNA (amino acids 439 to 636), or the human Kv1.4 cDNA (amino acids 601 to 655), or the human KvLQT1 (amino acids 367 to 676 of isoform 1) cDNA were cloned into pAdEcd-CD8trunc to generate pAdEcd-CD8-Kv4.3, pAdEcd-CD8-Kv1.4 and pAdEcd-CD8-KvLQT1.

Adenovirus vectors were generated by Cre-*lox* recombination of purified Ψ5 viral DNA and shuttle vector DNAs in CRE8 cells expressing the CRE recombinase (Hardy et al., 1997; Johns et al., 1999). The recombinant products were plaque-purified, expanded and purified on CsCl gradients yielding concentrations of the order of 10^{10} pfu/ml.

Cell Culture and Transduction

Epithelial Cells

OK cells were cultured in Dulbecco's modified Eagle medium: nutrient mixture F-12 (Ham) 1:1 (DMEM/F-12; Invitrogen, Carlsbad, CA) supplemented with 10% fetal bovine serum in the presence of penicillin and streptomycin and maintained at 37°C in 5% CO_2 in 75-cm^2 tissue culture flasks. For passage, the monolayers were rinsed twice with Hank's balanced salt solution (HBSS) without Ca^{2+} and Mg^{2+} (Invitrogen), and incubated with 0.25% trypsine-1 mM EDTA (Invitrogen) for 3 minutes. Cells were further dissociated mechanically and diluted 1 to 50 in new 75-cm^2 flasks. The medium was changed 3 times a week and cells passaged once a week.

For transduction, OK cells were trypsinized 4 days prior to transduction and plated at 50% confluence into 12-well Transwell® cell culture plates (Costar, Acton, MA). Cells were transduced two days after they reached confluence by adding 15 μl of each adenovirus in 0.5 ml of 10 μM-ponasterone A (an ecdysone analog; Invitrogen) in DMEM/F-12 per cluster. After 12 hours of incubation at 37°C, the medium was changed for 0.5 ml of fresh 10 μM-ponasterone A in DMEM/F-12. It was changed again after 24 hours in culture.

Cardiac Myocytes

Left ventricular myocytes from adult rats were isolated by Langendorff perfusion of the heart with collagenase type II (Worthington Biochemical, Lakewood, NJ) according to a protocol previously described (Neyroud et al., 2002). Freshly isolated myocytes were transduced in primary culture by adding 3 μl of each adenovirus to 1/10 of the cells in medium 199 (Invitrogen). After one hour of incubation at 37°C, myocytes were rinsed with medium 199 and cultured on 2% laminin (BD Biosciences, San Jose, CA) -coated cover-glasses in 10 μM-ponasterone A medium 199 supplemented with 2% fetal bovine serum in the presence of penicillin and streptomycin and maintained at 37°C in 5% CO_2 for 24 hours in 12-well plates.

Immunochemistry

Epithelial Cells

Fortyeight hours after transduction, OK cells plated in Transwell® clusters were stained with the Alexa Fluor® 488-conjugated wheat germ agglutinin (Molecular Probes, Eugene, OR), a lectin specific for the apical membrane, for 30 min on ice and fixed by 3% paraformaldehyde for 20 min on ice. Fixed cells were then permeabilized with 0.1% saponin-PBS for 10 min and blocked with 5% fetal bovine serum-1% bovine serum albumin-PBS for 30 min at room temperature, stained one hour with primary antibodies (1/50 dilution), rinsed with 0.1% saponin and stained one hour with secondary antibodies (1/100 dilution) and 5 μM DAPI in the dark.

The CD8-Kv channel fusion proteins were viewed with a mouse anti-human CD8 antibody (Sigma, St. Louis, MO) and with an Alexa Fluor® 568-conjugated anti-mouse antibody (Molecular Probes). The nucleus was imaged with the DAPI (Molecular Probes). The Grp78 protein, specifically expressed in the ER, was viewed with a rabbit anti-rat Grp78 antibody (StressGen Biotechnologies, Canada) and with an Alexa Fluor® 568-conjugated anti-rabbit antibody (Molecular Probes). Kv4.3 was imaged with a rabbit anti-rat Kv4.3 antibody (Alomone Labs, Israel) and with an Alexa Fluor® 568-conjugated anti-rabbit antibody (Molecular Probes).

Cardiac Myocytes

Twentyfour hours after transduction, cardiac myocytes were rinsed with PBS and stained alive with an R-Phycoerythrin-conjugated mouse anti-human CD8 antibody (1/50 dilution, Sigma, USA) for 20 min and rinsed again with PBS. Myocytes were then ready for patch-clamp experiments. For imaging, myocytes were fixed and stained like OK cells, but using a 10% goat serum-0.075% saponin-PBS solution for permeabilization, or a 5% fetal bovine serum-1% bovine serum albumin-PBS solution to block them without permeabilization. Staining was done with the same antibodies (and same concentrations) as for epithelial cells.

Confocal Microscopy

Images were taken on a laser confocal microscope (Zeiss LSM 410; Carl Zeiss, USA) with a 40× water immersion objective lens. GFP and Alexa Fluor® 488 were imaged with an Argon laser at 488 nm (excitation wavelength), Alexa Fluor® 568 with a green Helium-Neon laser at 543 nm and DAPI with an UV laser at 364 nm.

Electrophysiological Recordings

The whole-cell configuration of the patch-clamp technique (Hamill et al., 1981) was applied on rat ventricular myocytes 24 hours after transduction. The patch pipette contained (in mmol/1): 130 K-Glutamate, 9 KCl, 10 NaCl, 0.5 $MgCl_2$, 5 HEPES, 2 EGTA and 5 MgATP. The pH was adjusted to 7.2 with KOH. The bath solution contained (in mmol/1): 140 NaCl, 5 KCl, 0.1 $CaCl_2$, 1 $MgCl_2$, 10 HEPES and 10 glucose. The pH was adjusted to 7.4 with NaOH.

Experiments were performed at room temperature (22–23°C). Ionic currents were recorded with an Axopatch 200B patch-clamp amplifier (Axon Instruments, Foster City, CA) using low-resistance electrodes. Series resistance was compensated and currents were low-pass filtered at a cut-off frequency of 2 kHz. Currents, stimulus protocols and data collection were controlled by a microcomputer using Q software. Rat ventricular cell capacitance was assessed by applying a 10-mV hyperpolarizing pulse from a holding potential of −80 mV. The currents measured in myocytes were divided by the cell capacitance to express ionic current amplitudes as densities (pA/pF).

Statistical Analysis

Data are expressed as mean ± SEM. A 2-tailed Student's *t*-test was used to assess statistical significance when appropriate. Differences were considered to be significant at $P < 0.05$.

Results

Transduction of OK Cells

To investigate whether different Kv channels have distinct targeting determinants, it is necessary to analyze the subcellular localization of individual Kv channel subunits in a model system. We chose for this study OK cells, a cell line forming polarized, epithelial-like monolayers in culture. We first evaluated the ability of adenoviruses to transduce OK cells. Using an adenovirus concentration of $\sim 10^{10}$ plaque-forming units (pfu)/ml, we incubated cells with 0.5 μl to 30 μl adenovirus and we determined that 15 μl was the optimum amount of adenovirus to transduce OK cells. Moreover, cells had to be confluent for two days before transduction in order for the cell monolayer to be thick enough ($\sim$ 5 μm) to enable imaging on vertical cross sections with confocal microscopy.

Membrane Sorting of CD8 and CD8-Kv1.4 Proteins in OK Cells

OK cells were transduced with adenoviruses carrying the proteins CD8 or CD8-Kv1.4 and processed for immunofluorescence, utilizing the CD8 antibody. When observed in a plane parallel to the monolayer (Fig. 1*A*, top and bottom), the immunofluorescent signals from cells expressing the CD8 protein show a pattern characteristic of apical and basolateral membrane protein localization in epithelial cells. The punctate staining pattern on the apical surface of the monolayer images the membrane microvilli and is characteristic of apical labeling (top). The staining pattern surrounding each cell is typical of the lateral membrane (bottom). The same localization was observed for cells transduced with the AdEcdCD8-Kv1.4 adenovirus (Fig. 1*B*). Vertical cross-sectional projections of the images were constructed from stepwise scans perpendicular to the surface of the monolayer. The results of this analysis verify the apical and basolateral expression of both the CD8 and the CD8-Kv1.4 proteins in OK cells (Fig. 1*A* and 1*B*, lower panels).

Membrane Sorting of CD8-Kv4.3 and Kv4.3 Proteins in OK Cells

OK cells were transduced with an adenovirus carrying the fusion protein CD8-Kv4.3 and processed for immunofluorescence with the CD8 antibody. *En face* images show an apical and basolateral expression of the CD8-Kv4.3 protein (Fig. 2*A*). In order to compare the localization of this fusion protein, containing only the C-terminus of Kv4.3, with that of the full Kv4.3 protein, we transduced OK cells with AdEcdKv4.3 and processed them for immunofluorescence, utilizing the Kv4.3 antibody. Such cells show also the apical and basolateral patterns of expression, confirming that the C-terminal region of the protein suffices for fidelity of membrane targeting (Fig. 2*B*). Vertical cross-sectional projections of the monolayers verify the apical and basolateral expression of both the CD8-Kv4.3 and the full Kv4.3 proteins in OK cells (Fig. 2*A* and 2*B*, lower panels).

ER Retention of the CD8-KvLQT1 Fusion Protein in OK Cells

OK cells were transduced with an adenovirus carrying the fusion protein CD8-KvLQT1 and processed

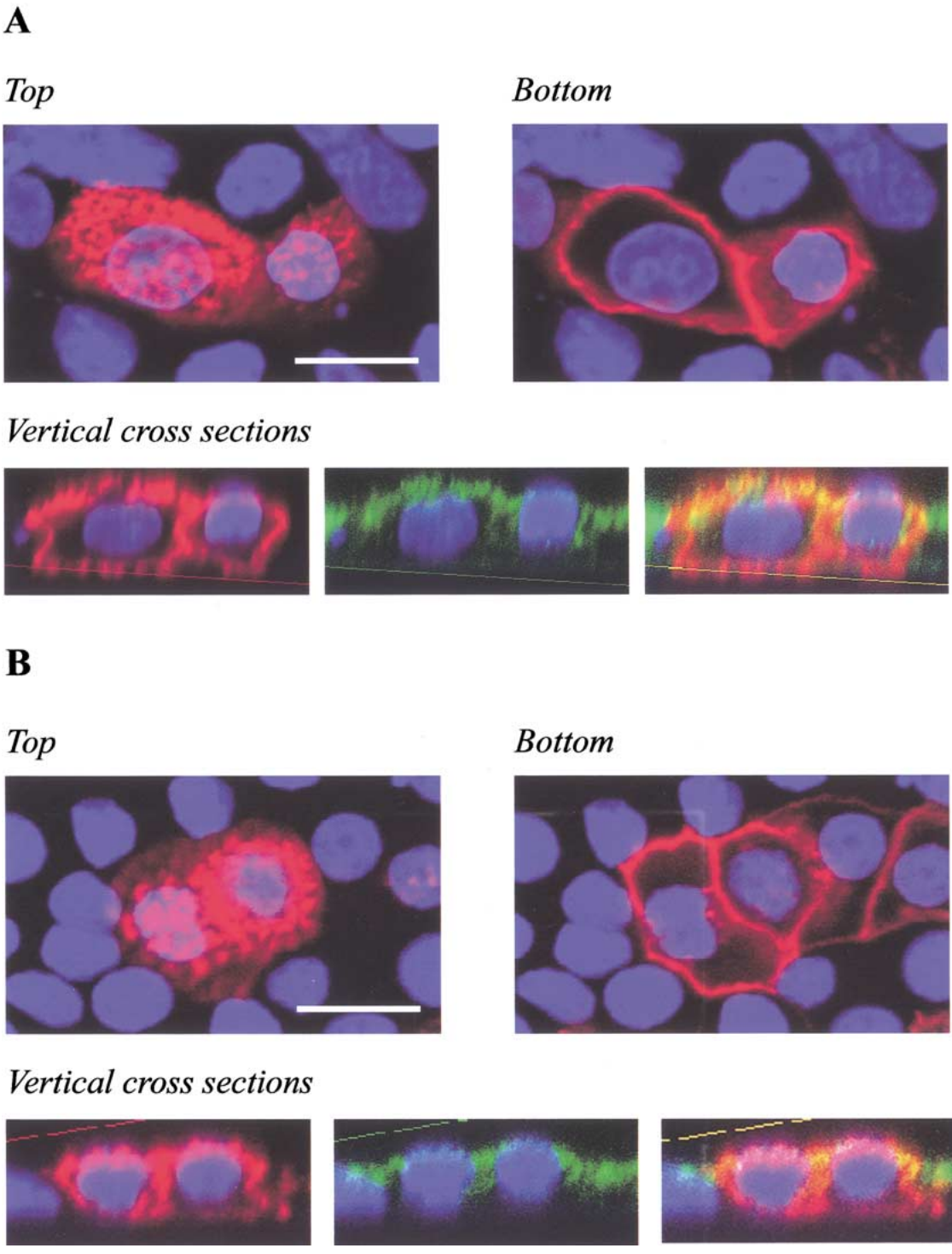

Fig. 1. CD8 and CD8-Kv1.4 localization in OK cells. Confocal images of OK cells transduced with AdEcd-CD8 (*A*) or AdEcd-CD8-Kv1.4 (*B*) after immunostaining with CD8 antibody (*red*). The DAPI (*blue*) stains the nucleus and the lectin (*green*) stains the apical membrane. (*Top* and *bottom*) *En face* images. (Vertical cross sections) Vertical cross-sectional projections of the monolayers: red fluorescence (*left*), green fluorescence (*middle*) and overlay (*right*). The vertical cross-sectional projections of the monolayers verify the apical and basolateral expressions of the CD8 and the CD8-Kv1.4 proteins. Scale bar: 15 μm.

for immunofluorescence utilizing the CD8 antibody. *En face* images show a pattern of expression completely different for CD8-KvLQT1 than for the previously-studied fusion proteins (Fig. 3*A*). The red fluorescence was restricted to an area surrounding the nucleus and is absent from either section of plasma

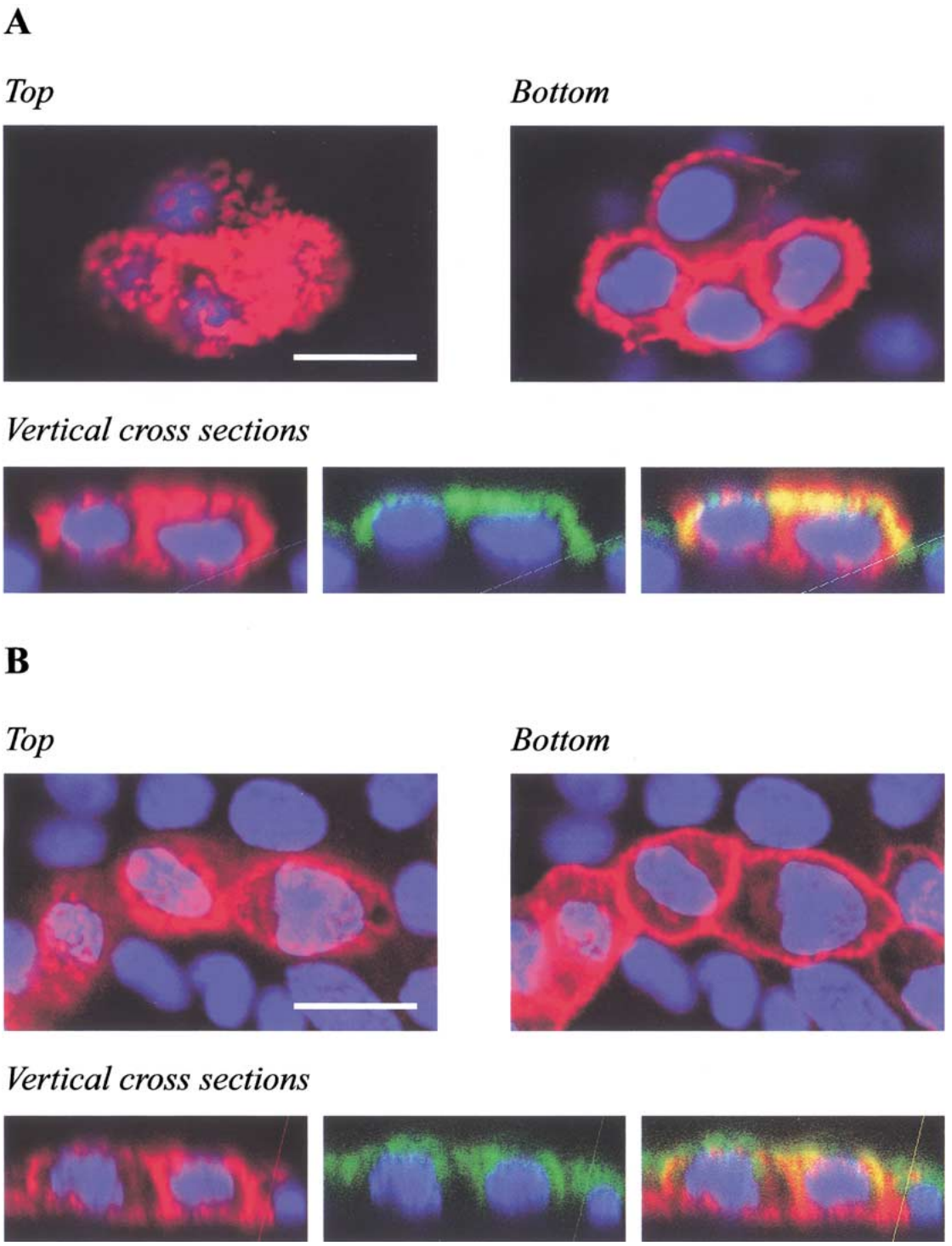

Fig. 2. CD8-Kv4.3 and Kv4.3 localization in OK cells. Confocal images of OK cells transduced with AdEcd-CD8-Kv4.3 (*A*) or AdEcd-Kv4.3 (*B*) after immunostaining with CD8 (*A*) or Kv4.3 (*B*) antibody (*red*). The DAPI (*blue*) stains the nucleus and the lectin (*green*) stains the apical membrane. (*Top* and *bottom*) *En face* images. (Vertical cross sections) Vertical cross sectional projections of the monolayers: red fluorescence (*left*), green fluorescence (*middle*) and overlay (*right*). The vertical cross sectional projections of the monolayers verify the apical and basolateral expressions of the CD8-Kv4.3 and Kv4.3 proteins. Scale bar: 15 μm.

membrane. This is shown by the absence of the punctate pattern of the apical surface and by the absence of staining of the lateral membrane visualized by the black line separating two transduced cells. We used the Grp78 protein as a control specific for the ER and showed that CD8-KvLQT1 had the same

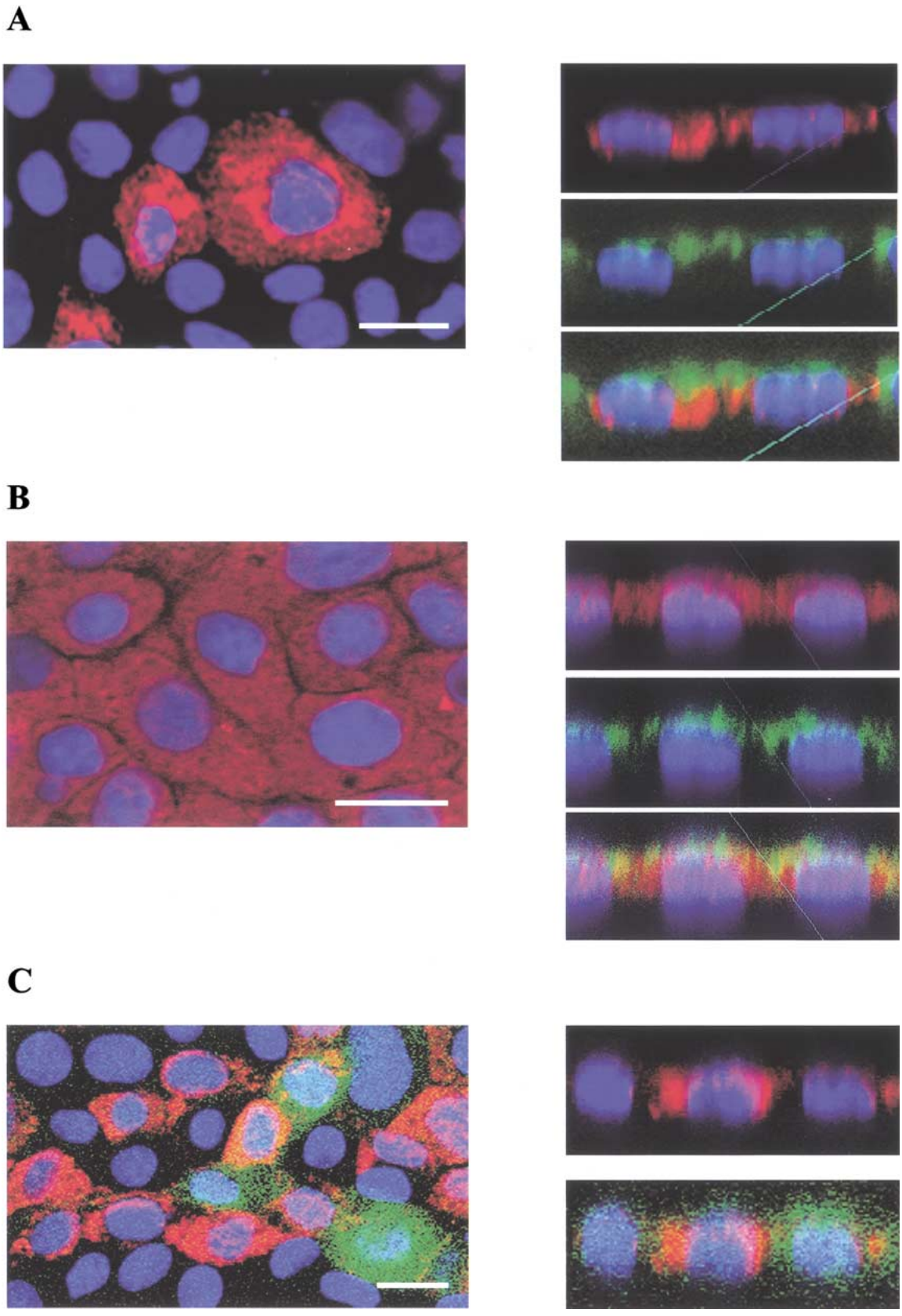

Fig. 3. CD8-KvLQT1 localization in OK cells. Confocal images of OK cells transduced with AdEcd-CD8-KvLQT1 (*A*) or AdEcd-CD8-KvLQT1 and AdCGI-MinK (*C*) after immunostaining with CD8 antibody (*red*). The DAPI (*blue*) stains the nucleus and the lectin (*green*) stains the apical membrane in *A* and *B*. In *C*, the green fluorescence (GFP) indicates cells transduced with AdCGI-MinK. Left hand side panels: *en face* images and right hand side panels: vertical cross sectional projections of the monolayers; red fluorescence (*top*), green fluorescence (*middle*) and overlay (*bottom*). The vertical cross sectional projections of the monolayers verify the ER retention of the CD8-KvLQT1 protein (*A*), even in presence of the MinK protein (*C*). Note that the Grp78 antibody (red), which stains the ER in control cells (*B*), is localized exactly where the CD8-KvLQT1 fusion protein is in transduced cells (*A*). Scale bar: 15 μm.

localization as Grp78 when overexpressed in OK cells (Fig. 3*B*). This reveals intracellular retention of the C-terminus of KvLQT1 when it is expressed alone (without the rest of the channel protein or accessory subunits) in epithelial cells. Vertical cross-sectional projections of the monolayers verify the ER retention of the CD8-KvLQT1 fusion protein, as it follows the pattern of expression of the endogenous Grp78 ER-specific protein in OK cells (Fig. 3*A* and 3*B*, right panels). There is no overlapping of the green apical staining and the red CD8-KvLQT1 protein, meaning that the fusion protein is not addressed to the apical membrane. The CD8-KvLQT1 protein is also absent from the basolateral membrane since there is no red staining of this membrane.

Since K^+-channel associating proteins, such as β-subunits, are known to facilitate the transfer of channel proteins from the ER to the plasma membrane, we overexpressed MinK (the principal KvLQT1 channel-associated protein) using the Ad-CGI-MinK adenovirus in cells transduced with CD8-KvLQT1. The presence of MinK was evidenced by the green fluorescence (GFP) and the presence of the CD8-KvLQT1 fusion protein by the red fluorescence (Fig. 3*C*). In cells showing both fluorescences, the localization of the CD8-KvLQT1 protein was unchanged compared to cells transduced with only AdEcd-CD8-KvLQT1. It was still retained in the ER. Vertical cross sectional projections of the monolayers verify the ER retention of CD8-KvLQT1 when expressed in the presence of MinK (Fig. 3*C*, right panels). Thus, MinK coexpression does not suffice to restore surface membrane targeting of the CD8-KvLQT1 construct.

Transduction of Heart Cells

The experiments conducted on polarized epithelial cells identified different targeting processes for different Kv channels. The CD8-Kv channel adenoviruses appeared to be well-designed to study subcellular processing of K^+ channels. We thus decided to reproduce this kind of experiment in heart cells. Figure 4 shows isolated adult rat ventricular myocytes transduced in culture with AdEcd-CD8-Kv4.3 and stained with an anti-CD8 antibody before (Fig. 4*A*) or after cell permeabilization (Fig. 4*B*). Such myocytes showed a high expression of CD8-Kv4.3 at the plasma membrane, even when the cells were permeabilized. Vertical cross-sections of the transduced myocytes verify the surface-membrane expression of CD8-Kv4.3 (Fig. 4, lower panels). We obtained the same results in myocytes transduced with AdEcd-CD8-Kv1.4 or AdEcd-CD8-KvLQT1 (*data not shown*). We then used this strong expression of the CD8-Kv4.3 fusion protein to the plasma membrane of myocytes to look for possible functional interactions between the Kv4.3 C-terminus and endogenous surrounding proteins in heart cells. For this purpose, we recorded ionic currents in cardiomyocytes transduced with the AdEcd-CD8-Kv4.3 adenovirus, looking for a modification of the endogenous I_{to}. We observed no t-tubules in these transduced cardiac myocytes kept for 24 hours in culture, in accordance with a previous report that t-tubules atrophy after 5 hours in primary culture (Lipp et al., 1996). Thus, no K^+ current was recorded from the t-tubule system in these cells.

Functional Consequences of CD8-Kv4.3 Overexpression in Ventricular Myocytes

Rat cardiac myocytes were transduced in culture with CD8-Kv4.3 or CD8 (as a control). Figure 5 shows records of the whole-cell I_{to} at different voltages in a cell expressing CD8 (Fig. 5*A*) and in a cell expressing CD8-Kv4.3 (Fig. 5*B*). Neither the peak current density (Fig. 5*C*) nor the half time of decay (Fig. 5*D*, 17.1 ± 2.1 msec in CD8 cells, $n = 13$ and 18.2 ± 1.8 msec in CD8-Kv4.3 cells, $n = 10$) was statistically different between CD8 myocytes and CD8-Kv4.3 myocytes, even though the peak current density tended to be smaller in CD8-Kv4.3 cells (7.43 ± 0.8 pA/pF, $n = 10$) than in CD8 cells (10.14 ± 1.96 pA/pF, $n = 13$). CD8-Kv4.3 overexpression did not affect the current-voltage relationship (Fig. 6*A*) or recovery from inactivation (Fig. 6*C*, $\tau_{rec}^{fast} = 21.5 \pm 5.3$ msec and $\tau_{rec}^{slow} = 257 \pm 68$ msec in CD8 myocytes, $n = 6$ and $\tau_{rec}^{fast} = 37.7 \pm 7.4$ msec and $\tau_{rec}^{slow} = 390 \pm 106$ msec in CD8-Kv4.3 myocytes, $n = 6$). However, the steady-state inactivation curve was significantly shifted in the hyperpolarizing direction (Fig. 6*B*, $V_{1/2} = -37.7 \pm 3$ mV and $k_v = 6.9 \pm 1$ in CD8 myocytes, $n = 6$ and $V_{1/2} = -47.9 \pm 2.4$ mV and $k_v = 9.4 \pm 0.8$ in CD8-Kv4.3 myocytes, $n = 5$; $p = 0.03$). Thus, the overexpression of Kv4.3 C-terminus in adult cardiac myocytes in culture specifically affects the voltage dependence of inactivation.

Discussion

The major results of this study are the following: (i) the use of polarized epithelial cells demonstrated different targeting processes of Kv-channels' C-termini, and (ii) the overexpression of Kv4.3 C-terminus in rat ventricular myocytes induced a shift of the steady-state inactivation curve towards negative potentials. We will discuss each of these results in turn.

One important finding of this study is that the C-terminus of KvLQT1 is not addressed to the plasma membrane of polarized cells, in contrast to Kv1.4 and Kv4.3 C-termini that are strongly expressed in this membrane. Membrane expression and localization of ionic channels are regulated by a variety of proteins

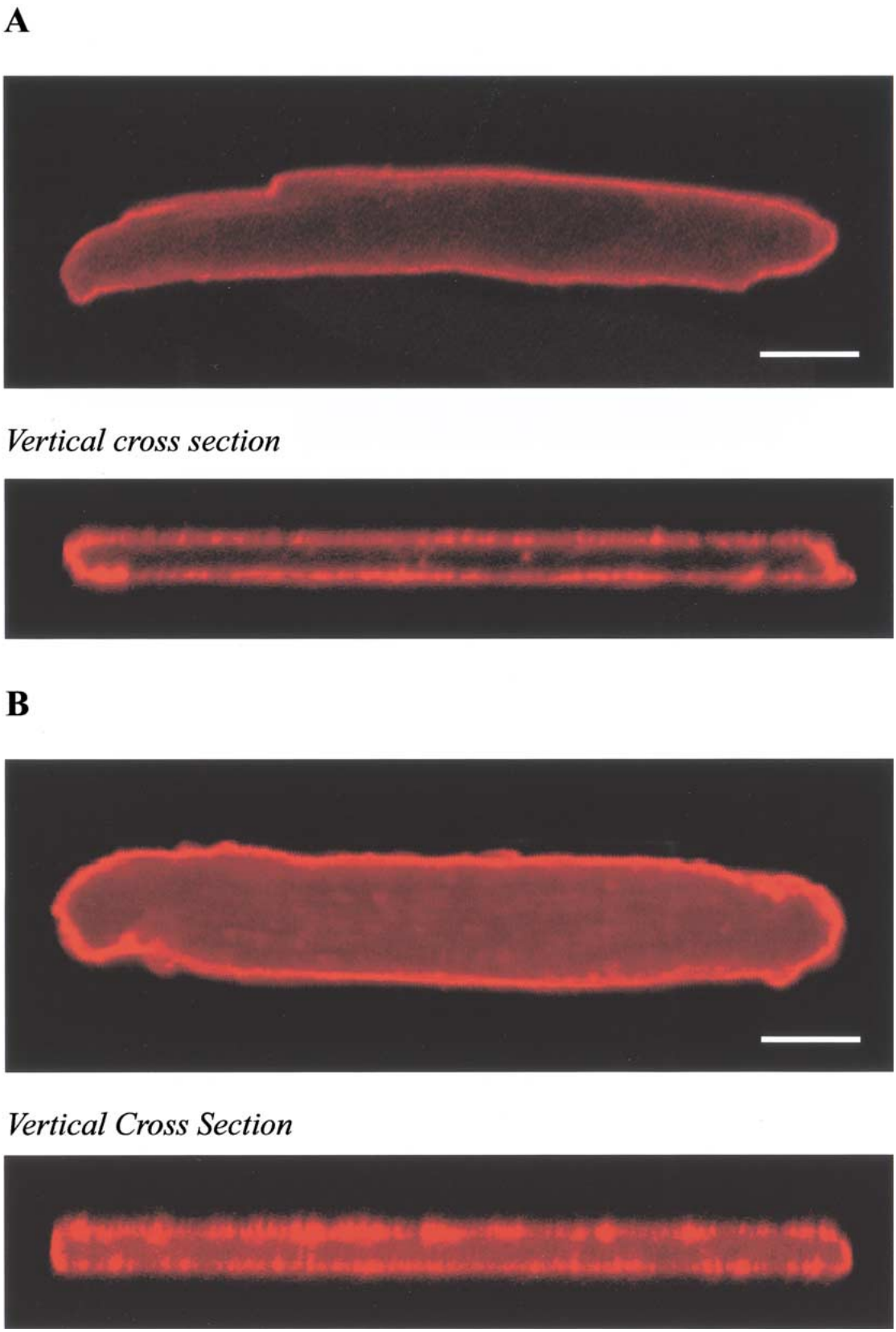

Fig. 4. CD8-Kv4.3 channel expression in cardiac myocytes. Confocal images of a non-permeabilized cardiac myocyte transduced with AdEcd-CD8-Kv4.3 (*A*) and a permeabilized one (*B*) after immunostaining with CD8 antibody (red fluorescence). Upper panels are *en face* images and lower panels are vertical cross sections of the myocytes. Note the strong expression of the CD8-Kv4.3 fusion protein on the plasma membrane of these cells, even when they were permeabilized to allow the antibody to reach intracellular proteins. Note also the absence of t-tubules in these myocytes cultured for 24 hours. Scale bar: 15 μm.

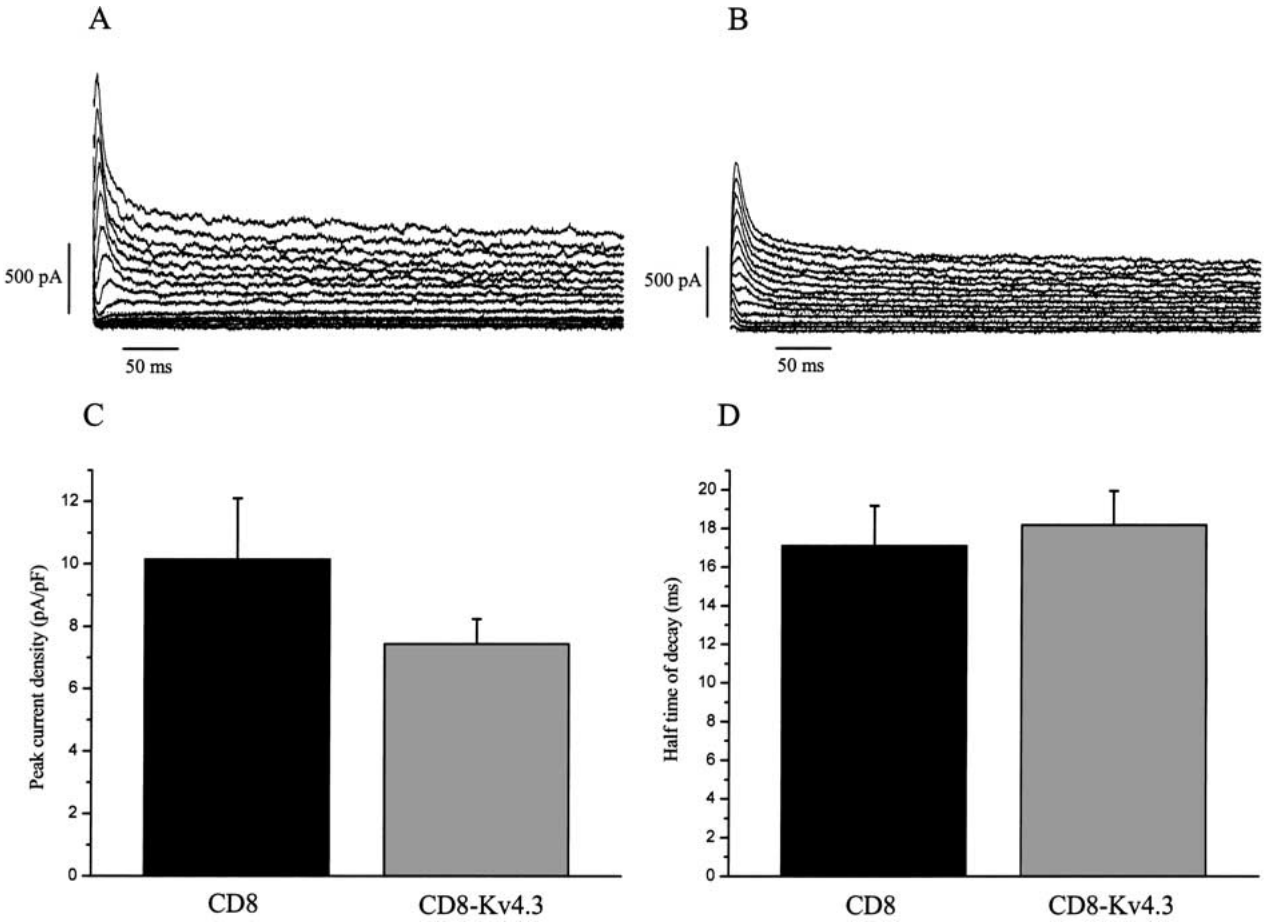

Fig. 5. Biophysical properties of CD8-Kv4.3 expressed in cardiac myocytes. Representative I_{to} currents in myocytes transduced with AdEcd-CD8 (*A*) or AdEcd-CD8-Kv4.3 (*B*). Currents were elicited by 500-msec voltage-clamp steps from −80 to 60 mV in 10-mV increments. (*C*) Peak current density in cells transduced with AdEcd-CD8 (*black bar*, $n = 13$) or AdEcd-CD8-Kv4.3 (*gray bar*, $n = 10$). Density of current was calculated by the subtraction of the steady-state current to the peak current divided by the cell capacitance, when myocytes were depolarized at 60 mV. The difference between cells transduced with AdEcd-CD8 and cells transduced with AdEcd-CD8-Kv4.3 was not statistically significant. Half time of decay (*D*) was the time where half of the peak current was decayed, when myocytes were depolarized at 60 mV. It was measured in 13 cells transduced with AdEcd-CD8 (*black bar*) and 10 cells transduced with AdEcd-CD8-Kv4.3 (*gray bar*). The difference was not statistically significant.

including the MAGUK proteins (for Membrane Associating GUanylate Kinase). These anchoring proteins show different capabilities to cluster and localize ionic channels to the plasma membrane. For instance, the MAGUK protein ZO-1 associates with connexins while PSD-95 and SAP-97 associate with Kir or Kv channels (Fujita & Kurachi, 2000). Moreover, the protein SAP-97 is selectively localized in the epithelial lateral membrane due to the presence of a distinct amino-acid sequence absent from other MAGUK proteins and allowing its association with specific cytoskeletal elements (Wu et al., 1998). Recently, it has been reported that epithelial cell polarity is also regulated by another MAGUK protein, the Stardust protein (Bachmann et al., 2001). Thus, it is likely that the C-terminus of KvLQT1 cannot associate with such anchoring proteins present in OK cells, while the C-termini of Kv1.4 and Kv4.3 channels can. This could result in the ER retention of CD8-KvLQT1 and the strong addressing of CD8-Kv1.4 and CD8-Kv4.3 to the plasma membrane. Likewise, the absence of a release of CD8-KvLQT1 from the ER by MinK eliminates a major role played by this ancillary protein in surface expression of the KvLQT1 channel in OK cells. Another reason for the CD8-KvLQT1 ER retention in OK cells could be that the fusion protein is not properly folded and is retained in the ER by quality control. Such a misfolding, due to the artificial fusion of CD8 with the KvLQT1 C-terminus, would expose the presence of a cell-type-specific ER-retention sequence in the KvLQT1 C-terminus. To our knowledge, there is no known ER-retention sequence in the C-terminus of KvLQT1 (e.g., the typical human KDEL retention signal (Pelham, 1990)), but it is possible that an as-yet-undefined C-terminal retention sequence is pres-

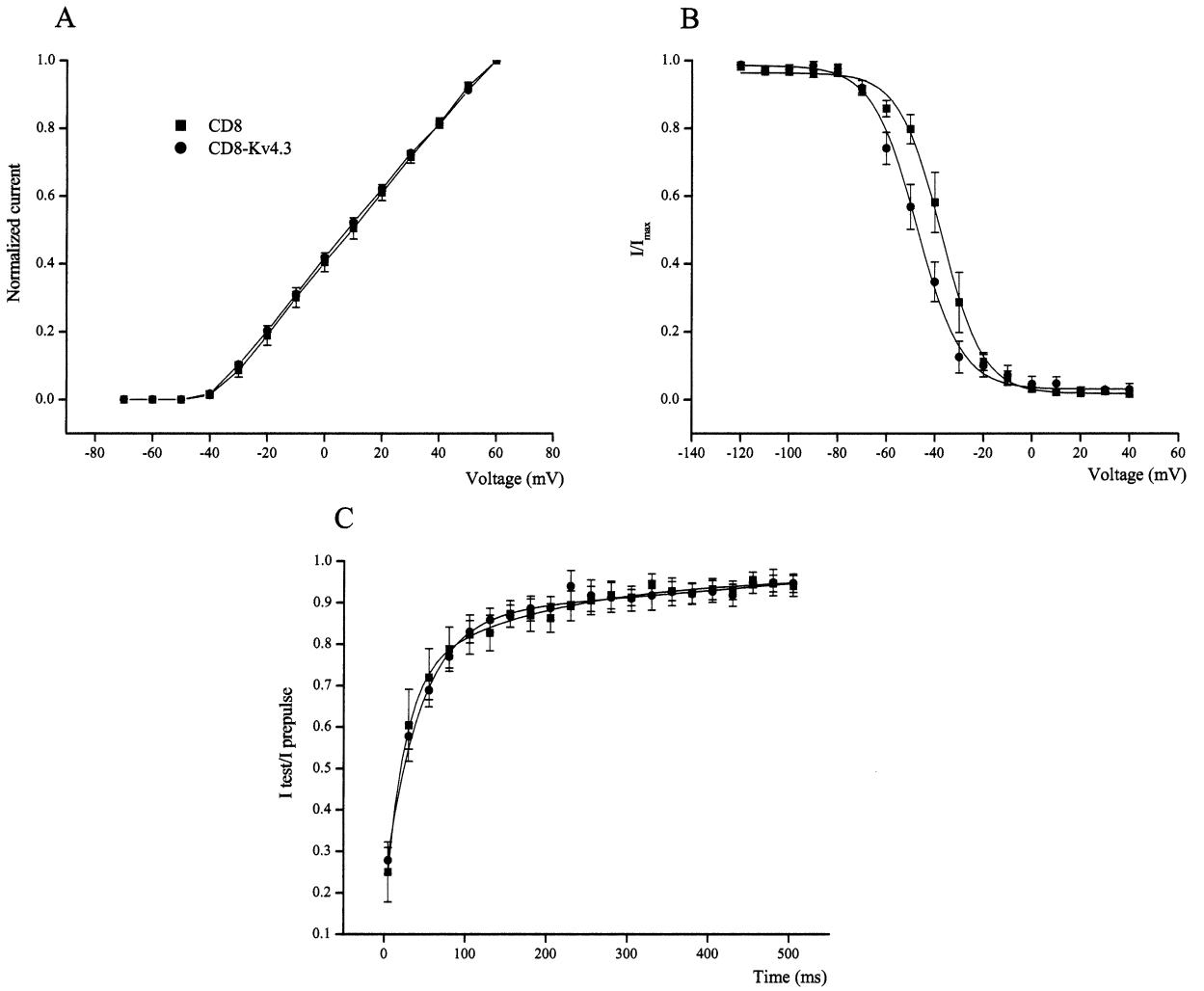

Fig. 6. Biophysical properties of CD8-Kv4.3 expressed in cardiac myocytes. (*A*) Normalized current-voltage (I/V) relationships elicited by 500-msec voltage-clamp steps from −80 to 60 mV in 10-mV increments (mean ± SEM) for cells transduced with AdEcd-CD8 (*squares*, $n = 6$) and cells transduced with AdEcd-CD8-Kv4.3 (*circles*, $n = 5$). (*B*) Voltage dependence of steady-state inactivation measured by a 2-pulse protocol with 1-sec conditioning pulses from −120 to 40 mV followed by a test pulse to 60 mV. The data were fit to a Boltzmann distribution. In cells transduced with AdEcd-CD8-Kv4.3 ($n = 5$), the steady-state inactivation curve was shifted by 10 mV in the hyperpolarizing direction compared with cells transduced with AdEcd-CD8 ($n = 6$; $p = 0.03$). (*C*) Recovery from inactivation elicited by a 500-msec prepulse to 60 mV with varying rest intervals at −80 mV followed by a 500-msec test pulse to 60 mV. It was measured in 6 cells transduced with AdEcd-CD8 and 6 cells transduced with AdEcd-CD8-Kv4.3.

ent and is responsible for ER retention in epithelial cells in case of misfolding of the KvLQT1 protein. On the other hand, our results do not exclude that a small fraction of the CD8-KvLQT1 construct reaches the OK cell membrane and that CD8-KvLQT1 ER retention images are the result of a control of the surface expression of KvLQT1 in epithelial cells. This would be concordant with the smaller K^+ current generally recorded with KvLQT1 than with Kv4.3 and Kv1.4 in mammalian cells. Moreover, the difference in K^+ currents would be the result of the difference in these channel C-termini.

Since Kv1.4 and Kv4.2 channels are addressed to axons and dendrites, respectively, in neurons and since OK cells reproduce neuronal subcellular localization (Dotti & Simons, 1990; Sheng et al., 1992), Kv1.4 was expected to be targeted to the apical membrane and Kv4.3 (which is very close to Kv4.2) to the basolateral membrane of epithelial cells. However, this study shows that CD8-Kv1.4 and CD8-Kv4.3 were both addressed to the apical and basolateral parts of the plasma membrane in OK cells. In order to confirm these results obtained with the C-terminus of Kv4.3, we expressed the full Kv4.3 protein in OK cells and demonstrated that it was also expressed in both the apical and the basolateral membranes. One reason may be that Kv4.3 (the cardiac channel) is subjected to different addressing processes than Kv4.2 (the neuronal channel). Alternatively, OK cells may not fully and accurately re-

produce neuronal subcellular localization. This might also explain why the CD8-Kv1.4 fusion protein reached both the apical and the basolateral membranes instead of the apical membrane, as might have been expected from the neuronal analogy. The ER retention of CD8-KvLQT1 in OK cells but not in cardiac myocytes reveals functional differences in trafficking between these two cell types. Altogether, these results demonstrate the important cell specificity of mechanisms that regulate subcellular localization of ionic channels.

In overexpressing Kv4.3 C-terminus in cardiac myocytes, we hypothesized that this C-terminus would interact with endogenous Kv-channel-associating proteins, capturing them from endogenous Kv4.3 channels and thus altering I_{to} in these cells. From this point of view, the stabilization of inactivation and the tendency to a lower current density observed in myocytes transduced with CD8-Kv4.3 could be explained by such an interaction. Yang et al. (2001) recently reported that Kvβ subunits increased expression of Kv4.3 channels by interacting with their C-termini in neurons. Expression of Kvβ subunits does not affect Kv4.3 channel gating but increases current density and protein expression. Moreover, this association between Kv4.3 and Kvβ subunits requires the C-terminus of the channel protein. It is thus very likely that the effect of CD8-Kv4.3 we observed in cardiac myocytes is due (at least in part) to an interaction between Kvβ subunit and the Kv4.3 C-terminus, this interaction impairing the endogenous association of Kvβ subunits with Kv4.3 channels. It is also conceivable that the hyperpolarizing shift of inactivation reflects an alteration of the channel tetramer composition in Kv4.3 subunits caused by the overexpression of Kv4.3 C-terminus. Such an effect on biophysical properties of heteromultimeric assembly has already been demonstrated with Kv1.x channels (Po et al., 1993). Although the exact mechanisms by which Kv4.3 C-terminus overexpression alters the transient outward current remain to be determined, our results indicate that it is possible to modulate endogenous K^+ currents in cardiac myocytes by adenoviral transfer of channel fragments that can modify channel function and expression. Such an approach may be useful to correct a defective channel, like mutated K^+ channels found in the long-QT syndrome (Ficker et al., 2000; Yamashita et al., 2001), by gene transfer.

In summary, we describe a gene transfer approach that is well-suited to investigate trafficking and function of defined segments of membrane proteins. The present method also offers a specific strategy for isolating accessory proteins: anti-CD8 affinity chromatography or immunoprecipitation could be used to purify physiological complexes, including components that may be associated with the expressed protein fragments. We have yet to exploit this feature of the approach, but its potential has not escaped our notice.

We thank Dr. M. Donowitz for the kind gift of the OK cells, and Dr. D.C. Johns for suggesting the experimental approach and for guidance with vector design. N.N. was partially supported by the Fondation Bettencourt and the Fondation Simone & Cino Del Duca. I.D. was a research fellow of the Heart and Stroke Foundation of Canada. M.A. was supported by the Banyu Fellowship in Cardiovascular Medicine. This work was supported by NIH/NHLBI Specialized Center of Research grant P50 HL52307 to E.M. and NIH grant RO1HL66381 to H.B.N.

References

Apkon, M., Nerbonne, J.M. 1991. Characterization of two distinct depolarization-activated K^+ currents in isolated adult rat ventricular myocytes. *J. Gen. Physiol.* **97:**973–1011

Bachmann, A., Schneider, M., Theilenberg, E., Grawe, F., Knust, E. 2001. Drosophila Stardust is a partner of Crumbs in the control of epithelial cell polarity. *Nature* **414:**638–643

Dotti, C.G., Simons, K. 1990. Polarized sorting of viral glycoproteins to the axon and dendrites of hippocampal neurons in culture. *Cell* **62:**63–72

Faivre, J.F., Calmels, T.P., Rouanet, S., Javre, J.L., Cheval, B., Bril, A. 1999. Characterisation of Kv4.3 in HEK293 cells: comparison with the rat ventricular transient outward potassium current. *Cardiovasc. Res.* **41:**188–199

Ficker, E., Dennis, A.T., Obejero-Paz, C.A., Castaldo, P., Taglialatela, M., Brown, A.M. 2000. Retention in the endoplasmic reticulum as a mechanism of dominant-negative current suppression in human long QT syndrome. *J. Mol. Cell. Cardiol.* **32:**2327–2337

Fujita, A., Kurachi, Y. 2000. SAP family proteins. *Biochem. Biophys. Res. Commun.* **269:**1–6

Hamill, O.P., Marty, A., Neher, E., Sakmann, B., Sigworth, F.J. 1981. Improved patch-clamp techniques for high-resolution current recording from cells and cell-free membrane patches. *Pfluegers Arch.* **391:**85–100

Hardy, S., Kitamura, M., Harris-Stansil, T., Dai, Y., Phipps, M.L. 1997. Construction of adenovirus vectors through Cre-*lox* recombination. *J. Virol.* **71:**1842–1849

Hille, B. 1992. Ionic channels of excitable membranes. Sinauer Associates, Massachusetts

Hoppe, U.C., Marbán, E., Johns, D.C. 2000. Molecular dissection of cardiac repolarization by in vivo Kv4.3 gene transfer. *J. Clin. Invest.* **105:**1077–1084

Hoppe, U.C., Marbán, E., Johns, D.C. 2001. Distinct gene-specific mechanisms of arrhythmia revealed by cardiac gene transfer of two long QT disease genes, *HERG* and *KCNE1*. *Proc. Natl. Acad. Sci.* **98:**5335–5340

Jang, S.K., Davies, M.V., Kaufman, R.J., Wimmer, E. 1989. Initiation of protein synthesis by internal entry of ribosomes into the 5′ nontranslated region of encephalomyocarditis virus RNA in vivo. *J. Virol.* **63:**1651–1660

Johns, D.C., Marx, R., Mains, R.E., O'Rourke, B., Marbán, E. 1999. Inducible genetic suppression of neuronal excitability. *J. Neurosci.* **19:**1691–1697

Li, D., Takimoto, K., Levitan, E.S. 2000. Surface expression of Kv1 channels is governed by a C-terminal motif. *J. Biol. Chem.* **275:**11597–11602

Lipp, P., Huser, J., Pott, L., Niggli, E. 1996. Spatially non-uniform Ca^{2+} signals induced by the reduction of transverse tubules in citrate-loaded guinea-pig ventricular myocytes in culture. *J. Physiol.* **497:**589–597

Neyroud, N., Nuss, H.B., Leppo, M.K., Marbán, E., Donahue, J.K. 2002. Gene delivery to cardiac muscle. *Methods Enzymol.* **346:**323–334

Pelham, H.R. 1990. The retention signal for soluble proteins of the endoplasmic reticulum. *Trends Biochem. Sci.* **15:**483–486

Pelletier, J., Sonenberg, N. 1988. Internal initiation of translation of eukaryotic mRNA directed by a sequence derived from poliovirus RNA. *Nature* **334:**320–325

Po, S., Roberds, S., Snyders, D.J., Tamkun, M.M., Bennett, P.B. 1993. Heteromultimeric assembly of human potassium channels. Molecular basis of a transient outward current? *Circ. Res.* **72:**1326–1336

Reshkin, S.J., Wuarin, F., Biber, J., Murer, H. 1990. Parathyroid hormone-induced alterations of protein content and phosphorylation in enriched apical membranes of opossum kidney cells. *J. Biol. Chem.* **265:**15261–15266

Rudy, B. 1988. Diversity and ubiquity of K channels. *Neuroscience* **25:**729–749

Sheng, M., Tsaur, M.L., Jan, Y.N., Jan, L.Y. 1992. Subcellular segregation of two A-type K^+ channel proteins in rat central neurons. *Neuron* **9:**271–284

Strang, C., Cushman, S.J., DeRubeis, D., Peterson, D., Pfaffinger, P.J. 2001. A central role for the T1 domain in voltage-gated potassium channel formation and function. *J. Biol. Chem.* **276:**28493–28502

Wickenden, A.D., Kaprielian, R., Kassiri, Z., Tsoporis, J.N., Tsushima, R., Fishman, G.I., Backx, P.H. 1998. The role of action potential prolongation and altered intracellular calcium handling in the pathogenesis of heart failure. *Cardiovasc. Res.* **37:**312–323

Wickenden, A.D., Kaprielian, R., Parker, T.G., Jones, O.T., Backx, P.H. 1997. Effects of development and thyroid hormone on K^+ currents and K^+ channel gene expression in rat ventricle. *J. Physiol.* **504:**271–286

Wu, H., Reuver, S.M., Kuhlendahl, S., Chung, W.J., Garner, C.C. 1998. Subcellular targeting and cytoskeletal attachment of SAP97 to the epithelial lateral membrane. *J. Cell Sci.* **111:**2365–2376

Yamashita, F., Horie, M., Kubota, T., Yoshida, H., Yumoto, Y., Kobori, A., Ninomiya, T., Kono, Y., Haruna, T., Tsuji, K., Washizuka, T., Takano, M., Otani, H., Sasayama, S., Aizawa, Y. 2001. Characterization and subcellular localization of KCNQ1 with a heterozygous mutation in the C terminus. *J. Mol. Cell Cardiol.* **33:**197–207

Yang, E.K., Alvira, M.R., Levitan, E.S., Takimoto, K. 2001. Kvbeta subunits increase expression of Kv4.3 channels by interacting with their C termini. *J. Biol. Chem.* **276:**4839–4844

Zito, K., Fetter, R.D., Goodman, C.S., Isacoff, E.Y. 1997. Synaptic clustering of Fascilin II and Shaker: essential targeting sequences and role of Dlg. *Neuron* **19:**1007–1016